Weak decays of beauty baryons at LHCb

Ulrik Egede, Monash University
On behalf of the LHCb collaboration

ICHEP
19 July 2024

Baryons with b quarks

- Electroweak penguin decays normally leads to the thought of B meson decays
  - $B^+ \to K^+ l^+ l^-$, $B^0 \to K^{*0} l^+ l^-$, $B^0_s \to \varphi l^+ l^-$, ...
  - $B^0 \to K^{*0}\gamma$, $B^0_s \to \varphi\gamma$, ...
- LHCb has in addition a very large sample of b baryons
  - This means that we get different angular structures in decay
  - Unfortunately Λ_b produced at the LHC are unpolarised at the percent level
  - Past measurements of $\Lambda_b \to \Lambda\mu^+\mu^-$, $\Lambda_b \to pK^-\mu^+\mu^-$, $\Lambda_b \to \Lambda\gamma$, $\Lambda_b \to pK^-\gamma$, ...

resonance	m_Λ [GeV/c^2]	Γ_Λ [GeV/c^2]	$2J_\Lambda$	P_Λ	$\mathcal{B}(\Lambda \to N\overline{K})$
$\Lambda(1405)$	1.405	0.051	1	−	0.50
$\Lambda(1520)$	1.519	0.016	3	−	0.45
$\Lambda(1600)$	1.600	0.200	1	+	0.15 – 0.30
$\Lambda(1670)$	1.674	0.030	1	−	0.20 – 0.30
$\Lambda(1690)$	1.690	0.070	3	−	0.20 – 0.30
$\Lambda(1800)$	1.800	0.200	1	−	0.25 – 0.40
$\Lambda(1810)$	1.790	0.110	1	+	0.05 – 0.35
$\Lambda(1820)$	1.820	0.080	5	+	0.55 – 0.65
$\Lambda(1890)$	1.890	0.120	3	+	0.24 – 0.36
$\Lambda(2110)$	2.090	0.250	5	+	0.05 – 0.25

New analysis of $\Lambda_b \to pK^- \mu^+ \mu^-$ decays

- Analysis based on full run 1 + run 2 dataset of 9 fb^{-1}
- Branching fraction and angular moments measured in bins of
  - q^2 (squared mass of leptonic system) and
  - m_{pK}^2 (squared mass of hadronic system)
- Branching fractions normalised to $\Lambda_b \to J/\psi p K^-$ decay
- 46 angular moments for unpolarised Λ_b

$$\frac{d^5\Gamma}{d\vec{\Phi}} = \frac{3}{8\pi} \sum_{i=1}^{46} K_i(q^2, m_{pK}^2) f_i(\cos\theta_\mu, \cos\theta_p, \phi)$$

JHEP 02 (2323) 189

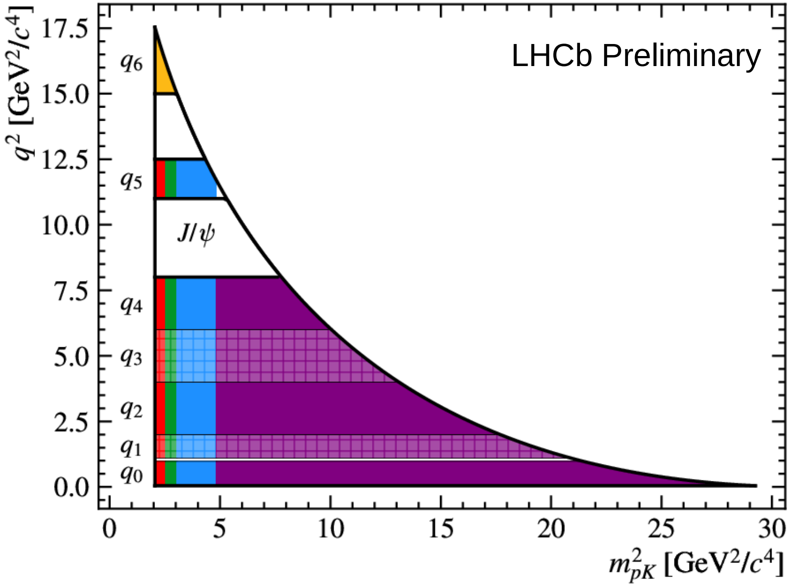

Selection of $\Lambda_b \rightarrow pK^-\mu^+\mu^-$

- Hardware trigger from muons, subsequent selection based on kinematics of tracks from displaced vertex and particle identification
- Veto on peaking backgrounds from mis-ID of hadrons (i.e. $B^0_s \rightarrow K^+K^-\mu^+\mu^-$)
- sPlot procedure with pKμμ mass used as discriminator between signal and background
- Signal regions chosen to avoid J/ψ and ψ(2S) contamination

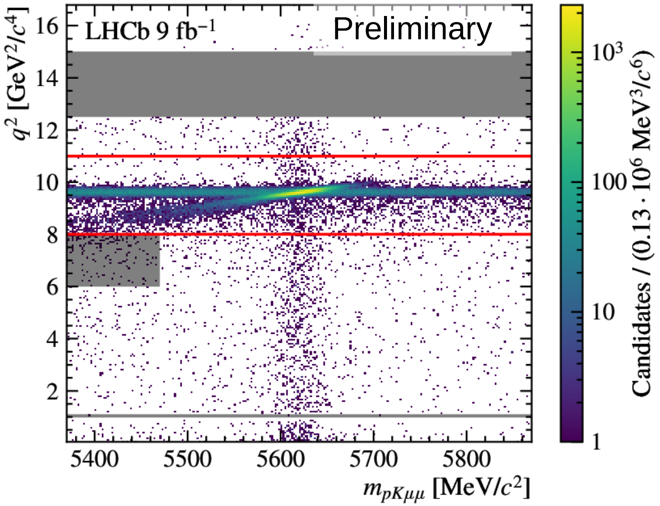

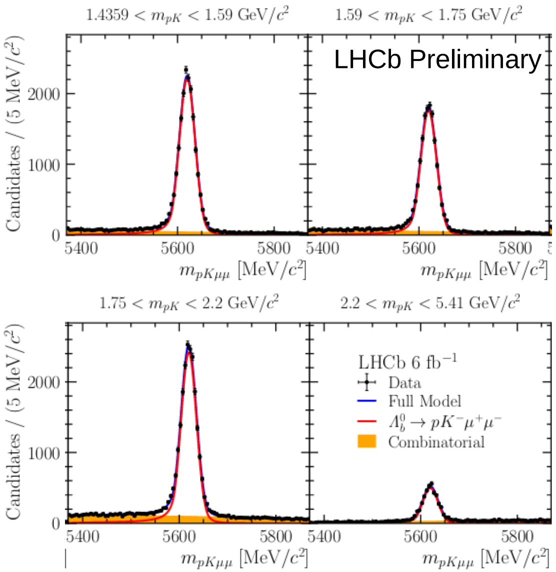

$\Lambda_b \to pK^- \mu^+ \mu^-$ signal

- Branching fraction determined in all bins, angular moments in bins with ★
  - Around 1000 signal candidates in total

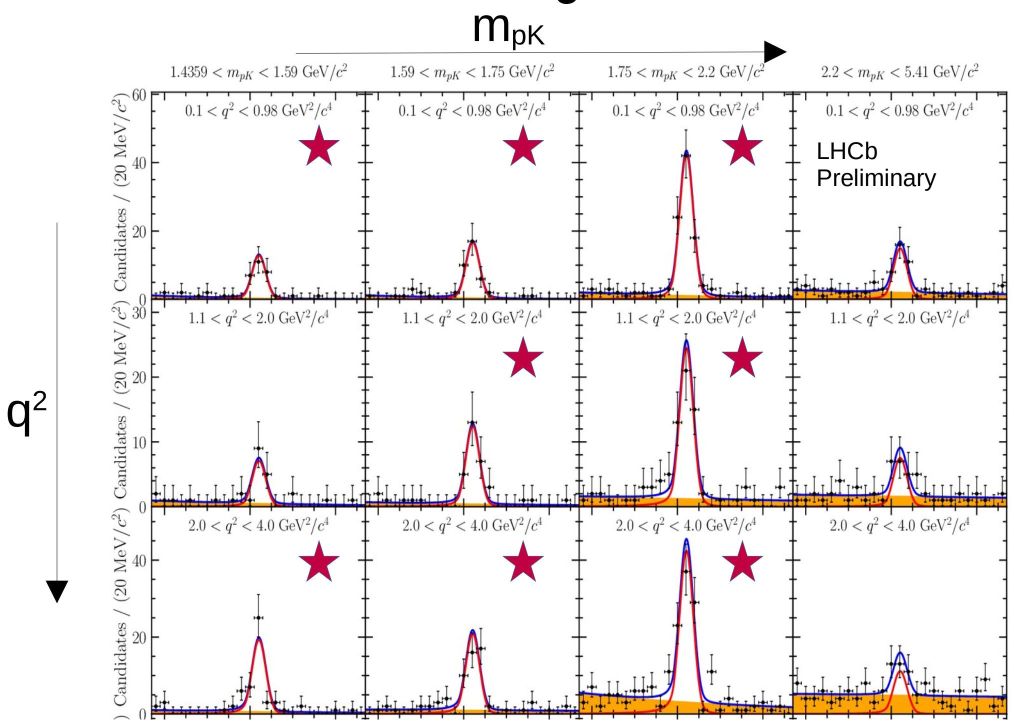

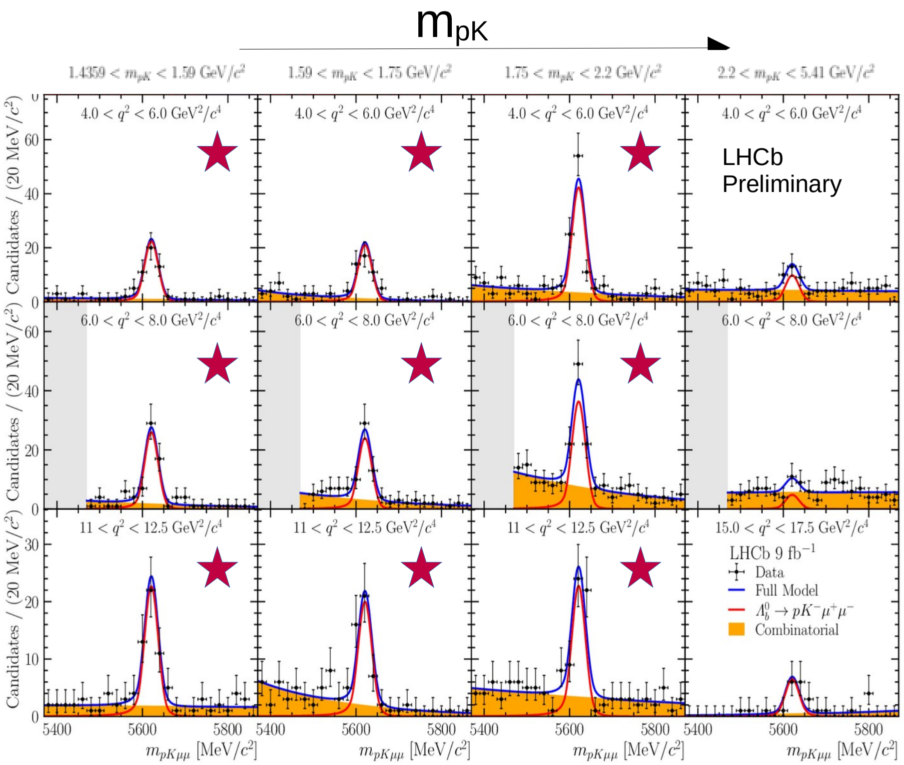

$\Lambda_b \to pK^- \mu^+ \mu^-$ branching fraction

- The signal yields from fit are converted to differential branching fractions using efficiency map and normalisation channel
  - Units of 10^{-8} GeV$^{-4}c^8$
  - Correlated normalisation dominates over other systematics

LHCb Preliminary

q^2 \ m_{pK}	$[1.4359, 1.59]$	$[1.59, 1.75]$	$[1.75, 2.2]$	$[2.2, 5.41]$
$[0.1, 0.98]$	$5.22 \pm 1.21 \pm 0.43 \pm 0.98$	$8.22 \pm 1.69 \pm 0.38 \pm 1.54$	$7.24 \pm 0.92 \pm 0.52 \pm 1.36$	$0.46 \pm 0.13 \pm 0.14 \pm 0.09$
$[1.1, 2.0]$	$3.05 \pm 1.45 \pm 0.51 \pm 0.57$	$6.27 \pm 1.71 \pm 0.40 \pm 1.18$	$4.24 \pm 0.78 \pm 0.16 \pm 0.80$	$0.16 \pm 0.09 \pm 0.02 \pm 0.03$
$[2.0, 4.0]$	$4.56 \pm 0.90 \pm 0.26 \pm 0.86$	$4.50 \pm 0.86 \pm 0.21 \pm 0.84$	$3.44 \pm 0.47 \pm 0.08 \pm 0.64$	$0.12 \pm 0.05 \pm 0.02 \pm 0.02$
$[4.0, 6.0]$	$4.72 \pm 0.76 \pm 0.15 \pm 0.89$	$4.29 \pm 0.73 \pm 0.20 \pm 0.81$	$3.36 \pm 0.41 \pm 0.07 \pm 0.63$	$0.11 \pm 0.03 \pm 0.02 \pm 0.02$
$[6.0, 8.0]$	$5.08 \pm 0.76 \pm 0.12 \pm 0.95$	$4.65 \pm 0.79 \pm 0.34 \pm 0.87$	$2.56 \pm 0.36 \pm 0.05 \pm 0.48$	$0.04 \pm 0.02 \pm 0.01 \pm 0.01$
$[11, 12.5]$	$5.32 \pm 0.86 \pm 0.20 \pm 1.00$	$4.53 \pm 0.80 \pm 0.16 \pm 0.85$	$1.67 \pm 0.28 \pm 0.03 \pm 0.31$	—
$[15.0, 17.5]$	$0.59 \pm 0.19 \pm 0.07 \pm 0.11$		—	—

Statistical Systematic Normalisation

$\Lambda_b \to pK^- \mu^+ \mu^-$ angular distributions

- Using sPlot weighted data and applying efficiency corrections gives pure weighted signal events *w(Φ)* in the 3D angular distribution
- Moments determined from weighted sum over basis functions

$$N = \sum_{\text{event } n} w(\vec{\Phi}_n) \qquad \overline{K}_i = \frac{1}{N} \sum_{\text{event } n} w(\vec{\Phi}_n) f_i(\vec{\Omega}_n)$$

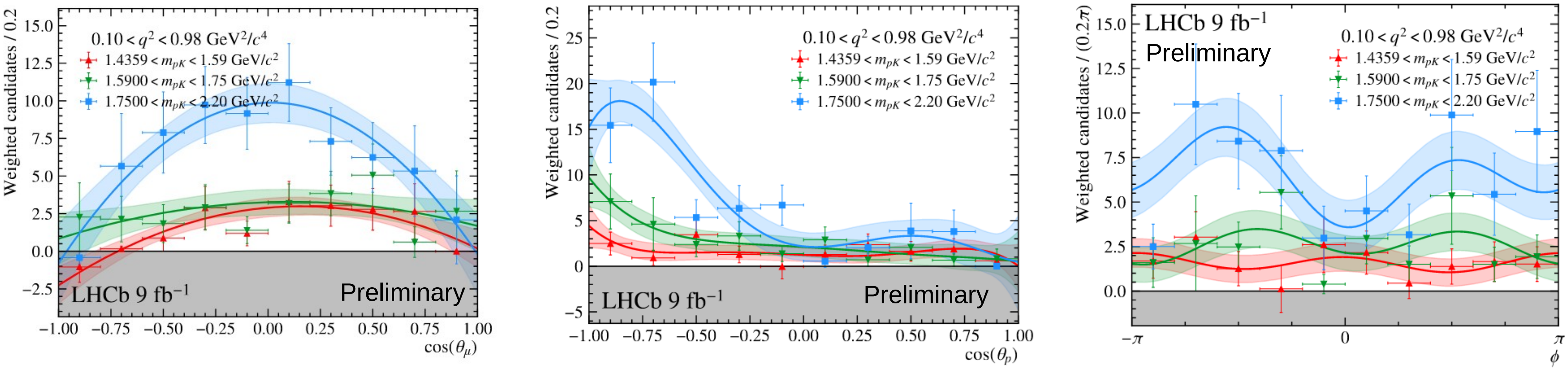

$\Lambda_b \to pK^- \mu^+ \mu^-$ hadronic interference

- Distribution in $\cos(\theta_p)$ is flat if there is only a contribution from a single hadronic resonance
  - Strong asymmetry in $1.75 < m_{pK} < 2.20$ GeV/c^2 bins

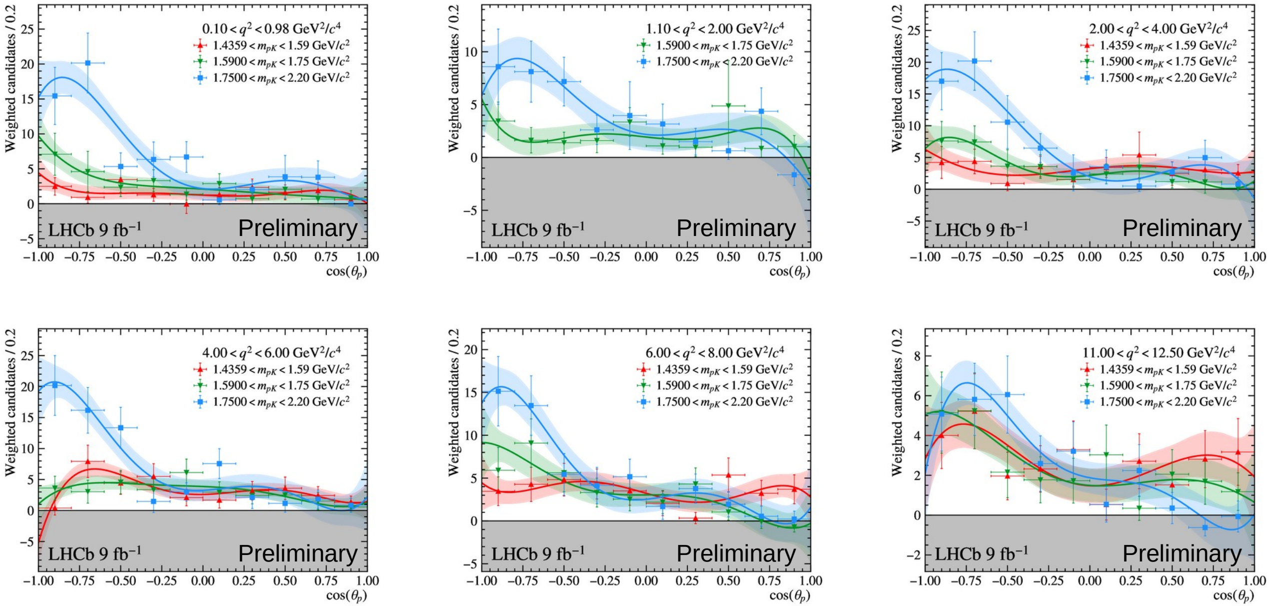

$\Lambda_b \to pK^-\mu^+\mu^-$ hadronic interference

- Distribution in $\cos(\theta_p)$ is flat if there is only a contribution from a single hadronic resonance
  - Strong asymmetry in $1.75 < m_{pK} < 2.20$ GeV/c^2 bins
- Implies interference of resonances with different parity

$$A_{FB}^{p} = \frac{3}{2}\overline{K}_4 - \frac{\sqrt{21}}{8}\overline{K}_{10} + \frac{\sqrt{33}}{16}\overline{K}_{16}$$

resonance	m_Λ [GeV/c^2]	Γ_Λ [GeV/c^2]	$2J_\Lambda$	P_Λ	$\mathcal{B}(\Lambda \to N\overline{K})$
$\Lambda(1405)$	1.405	0.051	1	−	0.50
$\Lambda(1520)$	1.519	0.016	3	−	0.45
$\Lambda(1600)$	1.600	0.200	1	+	0.15 – 0.30
$\Lambda(1670)$	1.674	0.030	1	−	0.20 – 0.30
$\Lambda(1690)$	1.690	0.070	3	−	0.20 – 0.30
$\Lambda(1800)$	1.800	0.200	1	−	0.25 – 0.40
$\Lambda(1810)$	1.790	0.110	1	+	0.05 – 0.35
$\Lambda(1820)$	1.820	0.080	5	+	0.55 – 0.65
$\Lambda(1890)$	1.890	0.120	3	+	0.24 – 0.36
$\Lambda(2110)$	2.090	0.250	5	+	0.05 – 0.25

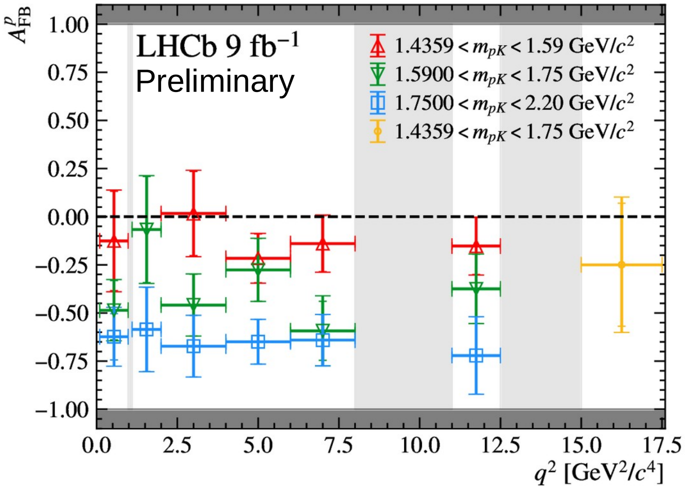

$\Lambda_b \to pK^- \mu^+ \mu^-$ leptonic A_{FB}

- Just as for B mesons, the forward-backward asymmetry of the leptons is sensitive to interference between Wilson coefficients C_7 and C_9
- Due to convention, the sign is flipped relative to A_{FB} for mesons

$$A^{\mu}_{\mathrm{FB}} = \frac{3}{2}\overline{K}_2$$

Predictions from JHEP 02 (2323) 189

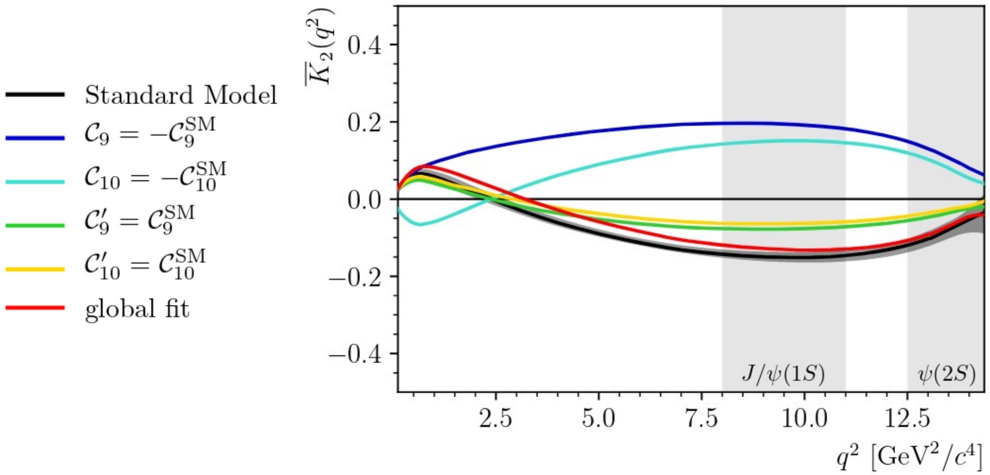

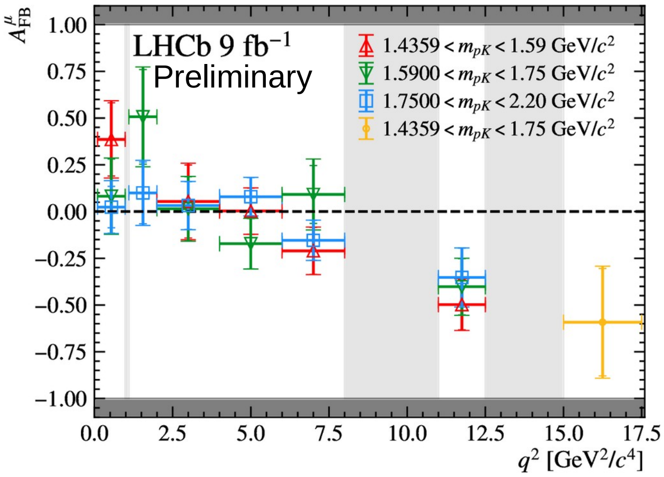

Hadronic interference

- While A_{FB} is sensitive to New Physics, other observables are uniquely sensitive to the hadronic interference

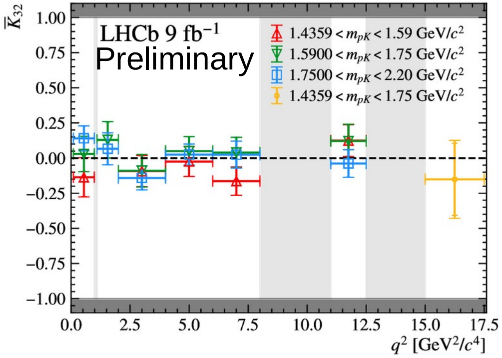

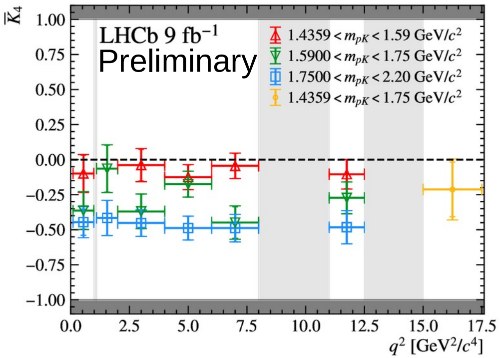

Predictions from JHEP 02 (2323) 189

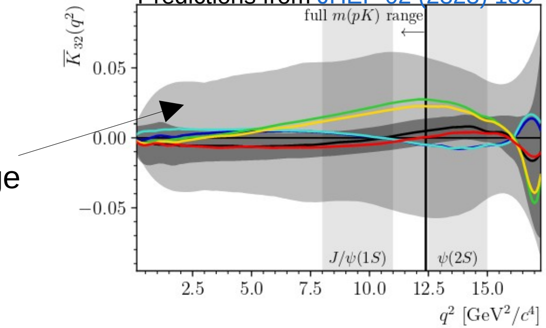

Band reflects change when changing interference

Predictions from JHEP 02 (2323) 189

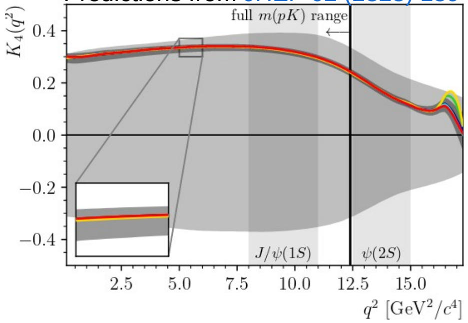

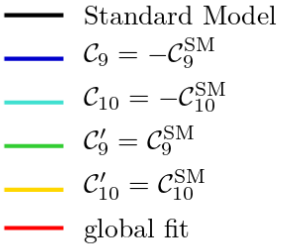

Comparison of hadronic spectra

- The hadronic mass spectra can be compared between $\Lambda_b \to pK^-\gamma$, $\Lambda_b \to pK^-\mu^+\mu^-$, and $\Lambda_b \to J/\psi pK^-$
  - Differences qualitatively align to expectations from available phase space

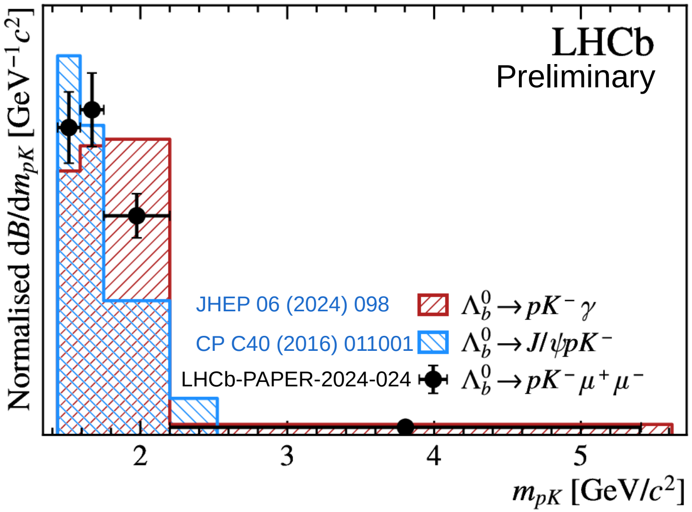

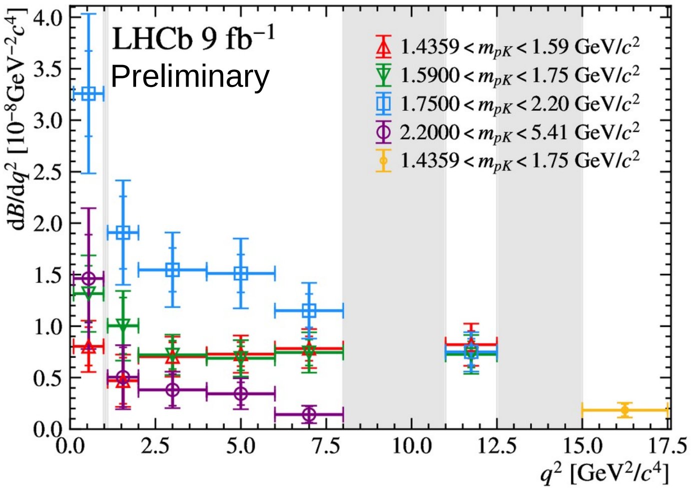

Conclusion

- In the $\Lambda_b \to pK^-\mu^+\mu^-$ final state there is a very rich structure with information in both the hadronic and leptonic system
  - A basis of 46 orthogonal moments for an unpolarised sample
  - Some moments sensitive to NP and some to hadronic system
- Further work to provide a full angular analysis of the $\Lambda_b \to \Lambda(1520)\mu^+\mu^-$ final state as well as a full decomposition of hadronic spectra

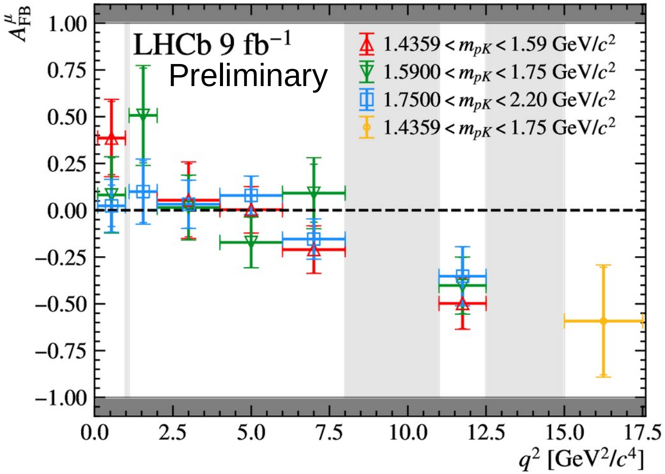

PRL 131, 151801 (2023)

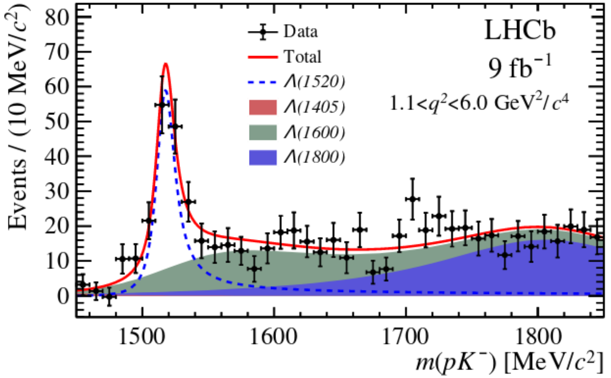

Backup

Orthogonal basis functions for moments

- Full list of eigenfunctions used for the moments
- $P^m_l(\cos\theta)$ are associated Legendre polynomials

i	$f_i(\vec{\Omega})$	i	$f_i(\vec{\Omega})$
1	$\frac{1}{\sqrt{3}}P_0^0(\cos\theta_p)P_0^0(\cos\theta_\mu)$	24	$\frac{1}{2}\sqrt{\frac{7}{3}}P_3^1(\cos\theta_p)P_1^1(\cos\theta_\mu)\cos\phi$
2	$P_0^0(\cos\theta_p)P_1^0(\cos\theta_\mu)$	25	$\frac{1}{2}P_4^1(\cos\theta_p)P_2^1(\cos\theta_\mu)\cos\phi$
3	$\sqrt{\frac{5}{3}}P_0^0(\cos\theta_p)P_2^0(\cos\theta_\mu)$	26	$\frac{3}{2\sqrt{5}}P_4^1(\cos\theta_p)P_1^1(\cos\theta_\mu)\cos\phi$
4	$P_1^0(\cos\theta_p)P_0^0(\cos\theta_\mu)$	27	$\frac{1}{3}\sqrt{\frac{11}{6}}P_5^1(\cos\theta_p)P_2^1(\cos\theta_\mu)\cos\phi$
5	$\sqrt{3}P_1^0(\cos\theta_p)P_1^0(\cos\theta_\mu)$	28	$\sqrt{\frac{11}{30}}P_5^1(\cos\theta_p)P_1^1(\cos\theta_\mu)\cos\phi$
6	$\sqrt{5}P_1^0(\cos\theta_p)P_2^0(\cos\theta_\mu)$	29	$\sqrt{\frac{5}{6}}P_1^1(\cos\theta_p)P_2^1(\cos\theta_\mu)\sin\phi$
7	$\sqrt{\frac{5}{3}}P_2^0(\cos\theta_p)P_0^0(\cos\theta_\mu)$	30	$\sqrt{\frac{3}{2}}P_1^1(\cos\theta_p)P_1^1(\cos\theta_\mu)\sin\phi$
8	$\sqrt{5}P_2^0(\cos\theta_p)P_1^0(\cos\theta_\mu)$	31	$\frac{5}{3\sqrt{6}}P_2^1(\cos\theta_p)P_2^1(\cos\theta_\mu)\sin\phi$
9	$\frac{5}{\sqrt{3}}P_2^0(\cos\theta_p)P_2^0(\cos\theta_\mu)$	32	$\sqrt{\frac{5}{6}}P_2^1(\cos\theta_p)P_1^1(\cos\theta_\mu)\sin\phi$
10	$\sqrt{\frac{7}{3}}P_3^0(\cos\theta_p)P_0^0(\cos\theta_\mu)$	33	$\frac{1}{6}\sqrt{\frac{35}{3}}P_3^1(\cos\theta_p)P_2^1(\cos\theta_\mu)\sin\phi$
11	$\sqrt{7}P_3^0(\cos\theta_p)P_1^0(\cos\theta_\mu)$	34	$\frac{1}{2}\sqrt{\frac{7}{3}}P_3^1(\cos\theta_p)P_1^1(\cos\theta_\mu)\sin\phi$
12	$\sqrt{\frac{35}{3}}P_3^0(\cos\theta_p)P_2^0(\cos\theta_\mu)$	35	$\frac{1}{2}P_4^1(\cos\theta_p)P_2^1(\cos\theta_\mu)\sin\phi$
13	$\sqrt{3}P_4^0(\cos\theta_p)P_0^0(\cos\theta_\mu)$	36	$\frac{3}{2\sqrt{5}}P_4^1(\cos\theta_p)P_1^1(\cos\theta_\mu)\sin\phi$
14	$3P_4^0(\cos\theta_p)P_1^0(\cos\theta_\mu)$	37	$\frac{1}{3}\sqrt{\frac{11}{6}}P_5^1(\cos\theta_p)P_2^1(\cos\theta_\mu)\sin\phi$
15	$\sqrt{15}P_4^0(\cos\theta_p)P_2^0(\cos\theta_\mu)$	38	$\sqrt{\frac{11}{30}}P_5^1(\cos\theta_p)P_1^1(\cos\theta_\mu)\sin\phi$
16	$\sqrt{\frac{11}{3}}P_5^0(\cos\theta_p)P_0^0(\cos\theta_\mu)$	39	$\frac{5}{12\sqrt{6}}P_2^2(\cos\theta_p)P_2^2(\cos\theta_\mu)\cos 2\phi$
17	$\sqrt{11}P_5^0(\cos\theta_p)P_1^0(\cos\theta_\mu)$	40	$\frac{1}{12}\sqrt{\frac{7}{6}}P_3^2(\cos\theta_p)P_2^2(\cos\theta_\mu)\cos 2\phi$
18	$\sqrt{\frac{55}{3}}P_5^0(\cos\theta_p)P_2^0(\cos\theta_\mu)$	41	$\frac{1}{12\sqrt{2}}P_4^2(\cos\theta_p)P_2^2(\cos\theta_\mu)\cos 2\phi$
19	$\sqrt{\frac{5}{6}}P_1^1(\cos\theta_p)P_2^1(\cos\theta_\mu)\cos\phi$	42	$\frac{1}{12}\sqrt{\frac{11}{42}}P_5^2(\cos\theta_p)P_2^2(\cos\theta_\mu)\cos 2\phi$
20	$\sqrt{\frac{3}{2}}P_1^1(\cos\theta_p)P_1^1(\cos\theta_\mu)\cos\phi$	43	$\frac{5}{12\sqrt{6}}P_2^2(\cos\theta_p)P_2^2(\cos\theta_\mu)\sin 2\phi$
21	$\frac{5}{3\sqrt{6}}P_2^1(\cos\theta_p)P_2^1(\cos\theta_\mu)\cos\phi$	44	$\frac{1}{12}\sqrt{\frac{7}{6}}P_3^2(\cos\theta_p)P_2^2(\cos\theta_\mu)\sin 2\phi$
22	$\sqrt{\frac{5}{6}}P_2^1(\cos\theta_p)P_1^1(\cos\theta_\mu)\cos\phi$	45	$\frac{1}{12\sqrt{2}}P_4^2(\cos\theta_p)P_2^2(\cos\theta_\mu)\sin 2\phi$
23	$\frac{1}{6}\sqrt{\frac{35}{3}}P_3^1(\cos\theta_p)P_2^1(\cos\theta_\mu)\cos\phi$	46	$\frac{1}{12}\sqrt{\frac{11}{42}}P_5^2(\cos\theta_p)P_2^2(\cos\theta_\mu)\sin 2\phi$

$\Lambda_b \to \Lambda(1520)\mu^+\mu^-$

- As all other electroweak penguin analyses, the normalisation of the branching fraction is done through the corresponding J/ψ decay mode

$$\left[\frac{d\mathcal{B}(\Lambda_b^0 \to \Lambda(1520)\mu^+\mu^-)}{dq^2}\right]_{q^2_{\rm min}}^{q^2_{\rm max}} = \frac{1}{(q^2_{\rm max}-q^2_{\rm min})}\frac{\mathcal{B}(\Lambda_b^0 \to pK^- J/\psi)\mathcal{B}(J/\psi \to \mu^+\mu^-)}{\mathcal{B}(\Lambda(1520) \to pK^-)} \times \frac{N_{\Lambda(1520)\mu^+\mu^-}}{N_{pK^-J/\psi}}\frac{\varepsilon_{pK^-J/\psi}}{\varepsilon_{\Lambda(1520)\mu^+\mu^-}},$$

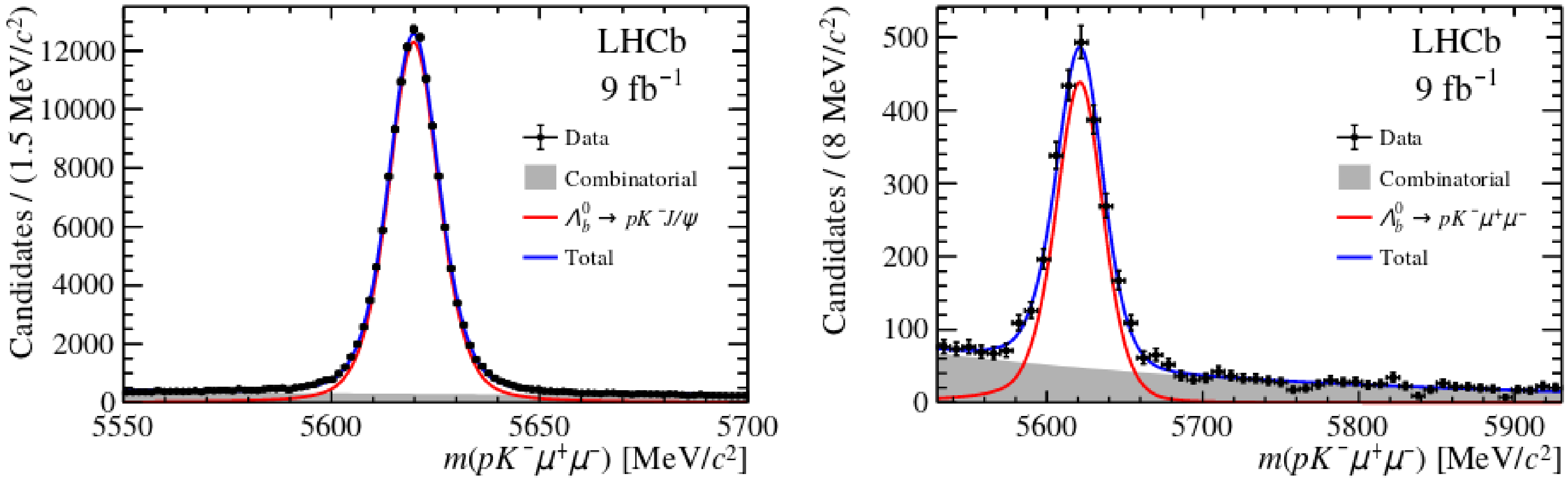

$\Lambda_b \to \Lambda(1520)\mu^+\mu^-$

- Fits of *pK*μμ mass distribution made in regions of q^2 outside the J/ψ and ψ(2S) resonances
- Very clear signal in all regions
- sWeights are then derived from this distribution to get the *signal only pK* mass distribution

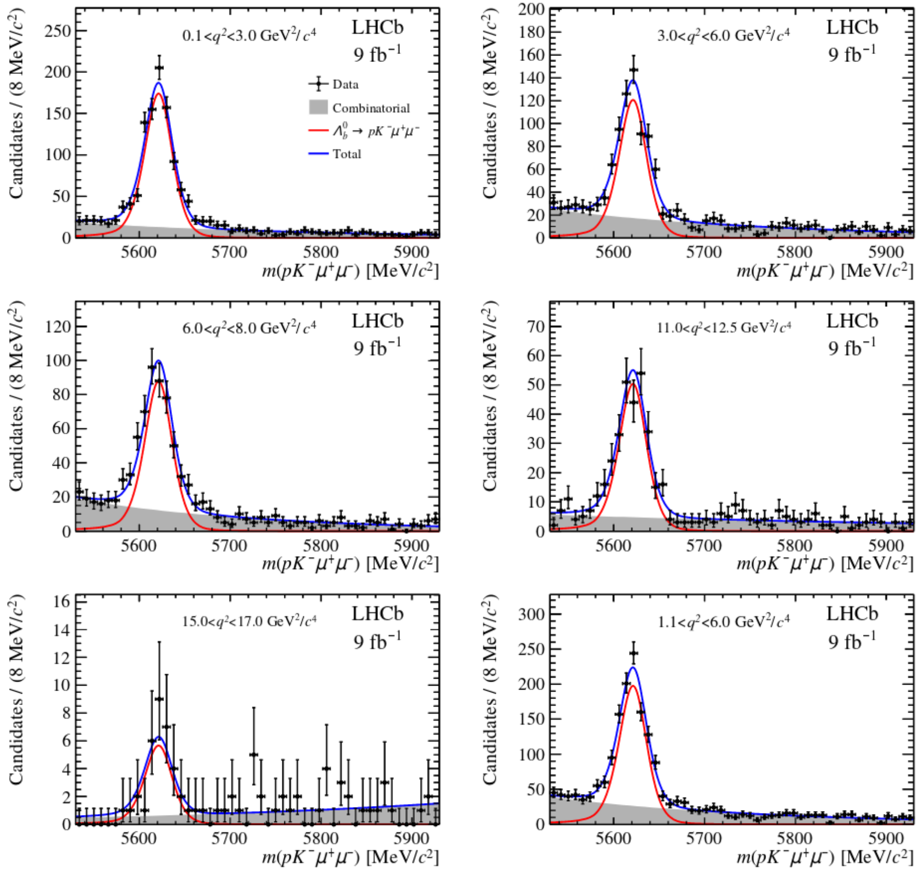

$\Lambda_b \rightarrow \Lambda(1520)\mu^+\mu^-$

- The $\Lambda(1520)$, $\Lambda(1405)$, $\Lambda(1600)$, and $\Lambda(1800)$ resonances all included in fit
- Relativistic Breit-Wigner lineshapes used
- Mass resolution so good that it only matters for $\Lambda(1520)$
- Uncertainty in resonance parameters and interference treated as systematics

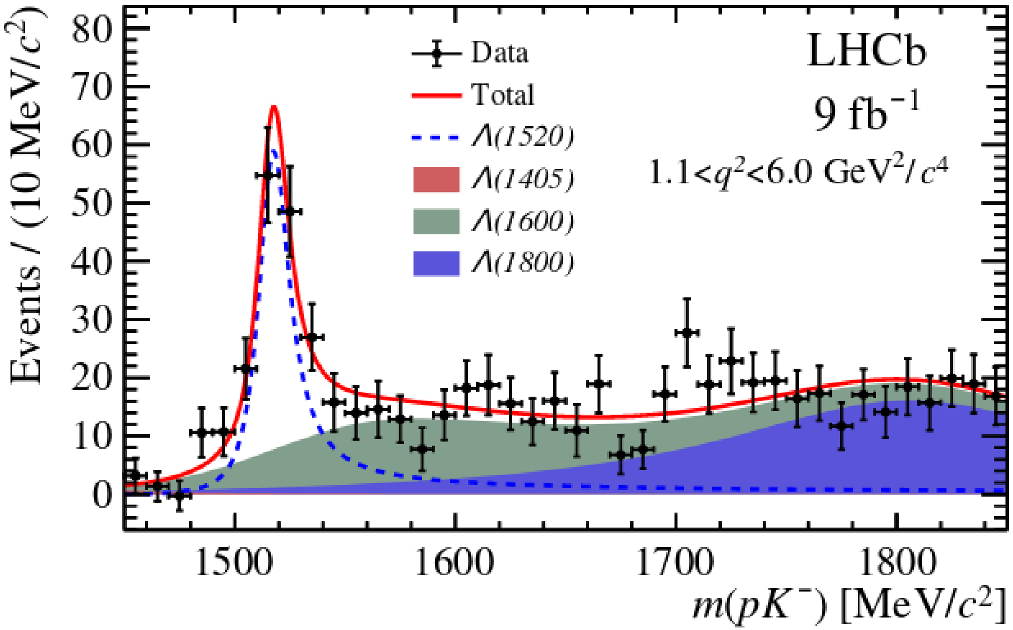

$\Lambda_b \to \Lambda(1520)\mu^+\mu^-$

- Fits in all regions show:
  - Clear Λ(1520) peak
  - Not as isolated as the K* in $B^0 \to K^{*0}\mu^+\mu^-$
  - Still promising for angular analysis

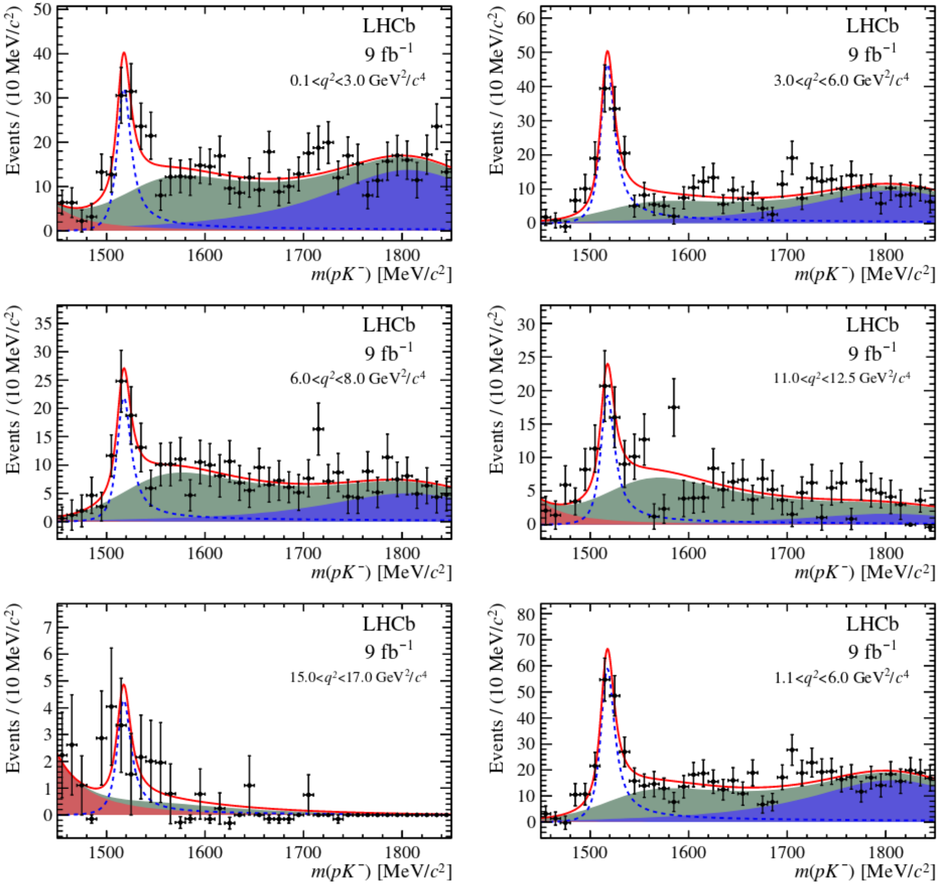

$\Lambda_b \rightarrow \Lambda(1520)\mu^+\mu^-$

- Branching fraction measurement at the end is dominated by statistical uncertainty
- Comparison to theoretical predictions are all over the place
- Some consolidation required on theory side to be conclusive

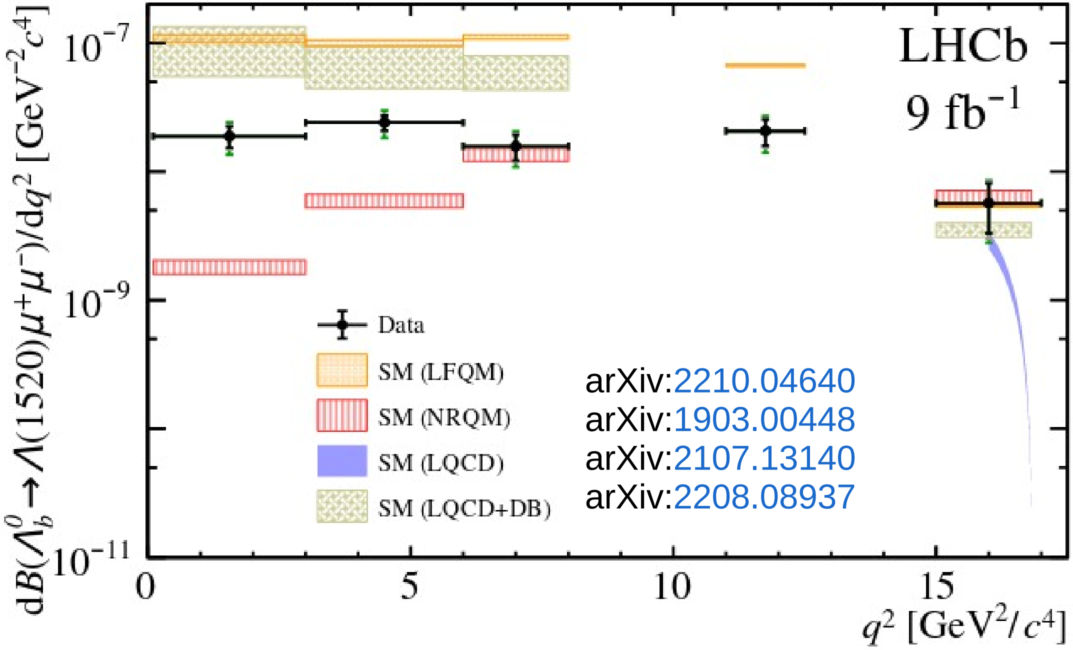

arXiv:2210.04640
arXiv:1903.00448
arXiv:2107.13140
arXiv:2208.08937